

Modelling and simulation of the machining process based on multiscale approach – a comprehensive review

Modelowanie i symulacja procesu obróbki na podstawie podejścia wieloskalowego – przegląd

WIT GRZESIK
KRZYSZOF JAROSZ *

DOI: <https://doi.org/10.17814/mechanik.2025.7.6>

This paper reviews key principles of multiscale modeling and numerical simulations of fundamental physical phenomena in machining processes, including plastic deformation, chip formation, and interfacial friction. Representative applications of modeling for multiphase and composite materials, determination of constitutive equation constants, and simulation of nano- and micromachining processes using hybrid MD+FEM and SPH+FEM methods are discussed.

KEYWORDS: multiscale modeling, FEM, MD, SPH, machining simulation, micro/nanomachining

W artykule przedstawiono kluczowe zasady modelowania wieloskalowego oraz symulacji numerycznych zjawisk fizycznych zachodzących w procesach obróbki skrawaniem, takich jak odkształcenia plastyczne, powstawanie wiórów i tarcie międzyfazowe. Omówiono wybrane przykłady zastosowania modelowania do materiałów wielofazowych i kompozytowych, wyznaczania stałych w równaniach konstytutywnych materiału oraz symulacji procesów nano- i mikroobróbki przy użyciu metod hybrydowych MD+FEM i SPH+FEM.

SŁOWA KLUCZOWE: modelowanie wieloskalowe, symulacja obróbki, mikroobróbka, nanoobróbka

Introduction

Multiscale modelling techniques are powerful tools for bridging the multiple scales shown in fig. 1, capable of relating macroscopic material behaviour to microscale features and mechanisms. In this way, they can be used for numerous advanced modelling and simulation applications in solid mechanics.

Applications of multiscale modelling include not only the design of materials with optimal structure and properties, including composite materials reinforced with nanoparticles (FRP), but also manufacturing processes, including additive forming using the SLM method, plastic and subtractive processing, even on the micro and nano scale. [1, 2, 3, 4]. In turn, numerical simulation using hybrid methods, such as those based on combining molecular dynamics (MD) with the finite element method (FEM) in a two-scale model (MD+FEM), help to solve the important problem of time-consuming calculations, which commonly occurs when using a uniform finite element mesh with a very small mesh element dimension [1, 4, 5].

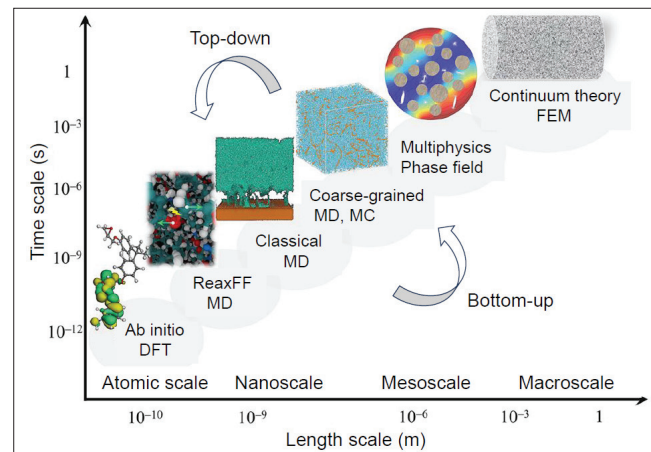


Fig. 1. Diagram showing applications of different modeling methods in the continuum solid mechanics in the time-length scale coordinate system [1]

Fig. 1 presents an overview of modelling and simulation methods in the time-length system, starting from the atomic scale (comparable with atomic constant) through the nanoscale and mesoscale, up to the macroscale for which the dimension is higher than 10^{-3} m. These are the follows: AIMD - *Ab initio* (from first principles) molecular dynamics, DFT (*density functional theory*), ReaxFF MD (*reactive force-field MD*), classical (deterministic) MD method, classical (stochastic) Monte Carlo (MC) method, phase field method and FEM. DFT/MD (*Ab initio molecular dynamics*) is used to calculate the forces between atoms at each time step. MD and MC methods, on the other hand, are used in computer simulation of multimolecular systems. In both cases, these are problems of quantum and molecular chemistry. It should be noted that modelling can be performed in two ways, namely down-scale (*top-down*) and up-scale [5].

Modelling and simulation of the behaviour of the workpiece material and tool

Microstructure modelling can include both the machined material and the tool to determine their behaviour under mechanical and thermal loads. This is crucial for increasing the accuracy of numerical simulations of cutting processes, especially for multiphase materials. Such materials, like WC-Co cemented carbides, have properties that strongly depend on internal

* Prof. dr hab. inż. Wit Grzesik – wit.grzesik@gmail.com, <https://orcid.org/0000-0003-3898-5119> – Opole, Polska
PhD Candidate Krzysztof Jarosz – Rochester Institute of Technology, USA (corresponding author)

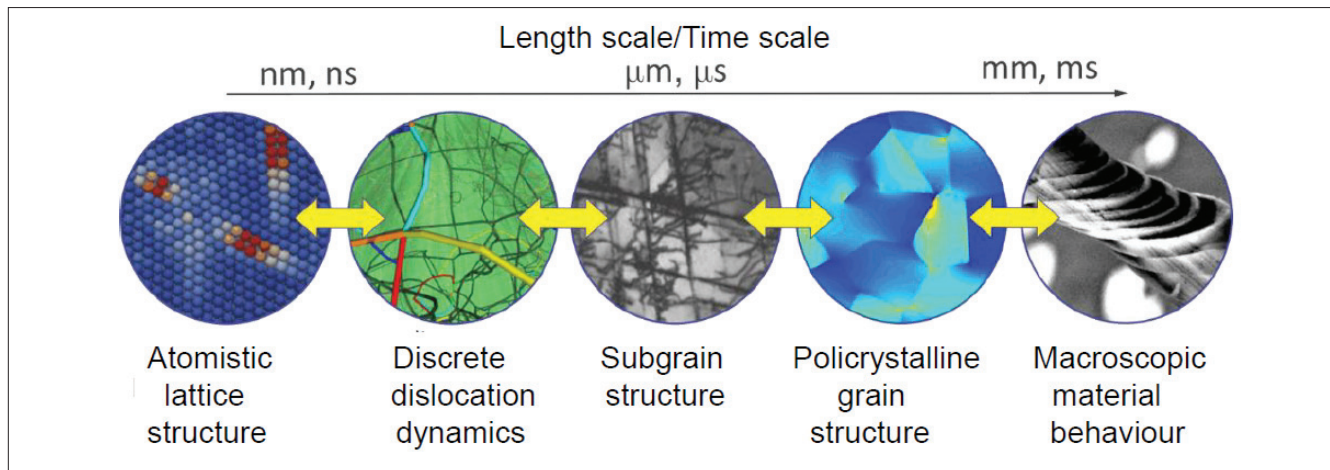


Fig. 2. Comparison of material structure length/time scales [16]

microstructure features, such as grain size, shape, distribution of the constitutive phases, and interphase features. Fig. 2 shows the successive stages in the multiscale analysis of the material's microstructure, from the nanometric atomic grid to the millimetre-scale macroscopic material.

Examples of material microstructure models determined by numerical modelling are shown in fig. 3. In the case of materials with a polycrystalline (multiphase) structure, a modified method for homogeneous materials (RVE–representative volume element) replicates the real microstructure mapped by scanning electron microscopy (SEM) or inverse electron diffraction (EBSD–backscattering diffraction). Another approach uses various statistical and numerical methods, such as Voronoi tessellations, the synthetic grain structure builder (DREAM.3D), Monte Carlo (MC), and CCBuilder [2, 6]. This creates a synthetic structure from a 2D image of the real microstructure (fig. 3a). For the WC-10% Co wt. carbide microstructure in fig. 3b, the Automatic Reconstruction (MIPAR™) method was used for image analysis and segmentation, and special learning algorithms (Pulse-coupled neural networks (PCNN)) were employed to generate a FEM [2, 6].

Metallic materials with a polycrystalline structure (i.e. composed of single crystals of single crystals) are most often subjected to machining, as shown in fig. 2. Their plastic deformation can occur by sliding

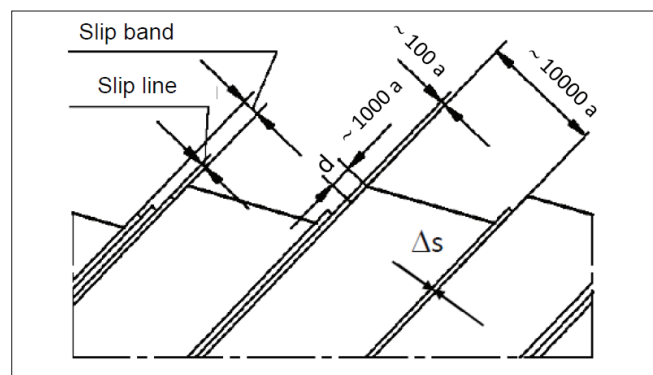


Fig. 4. Schematic of the shear phenomenon and shear band displacement at the outer chip surface; symbols: a – atomic lattice constant, d – displacement of the shear band, Δs – width of the shear band [5]

and twinning [5]. It should be noted that slip develops gradually and starts successively in the planes and directions where the shear stress first reaches, i.e. the yield point in shearing. However, due to its anisotropy, it can occur at lower shear stress values in the so-called easy slip systems. The effects of plastic deformation at the microstructure scale are visible in the form of slip bands, consisting of a series of slip lines, as shown in fig. 4.

Due to the presence of linear defects known as dislocations in the crystal lattice, slip occurs when the shear yield stress is several orders of magnitude lower. For example, for pure iron, the corresponding

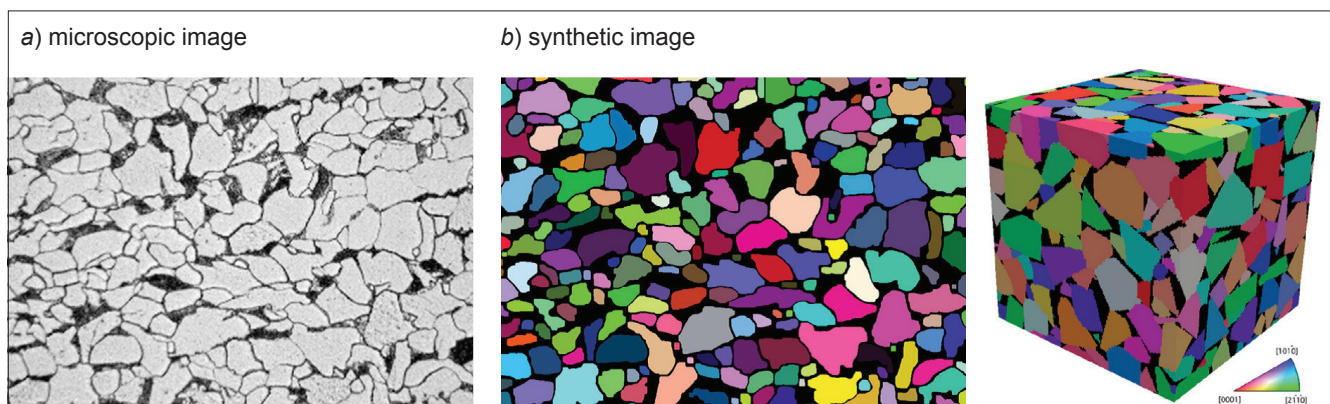


Fig. 3. Examples of the DMR obtained based on the optical microscopy image of a two phase steel (a) and synthetic microstructures generated for WC/Co-10 Co wt % (b) [2, 6]

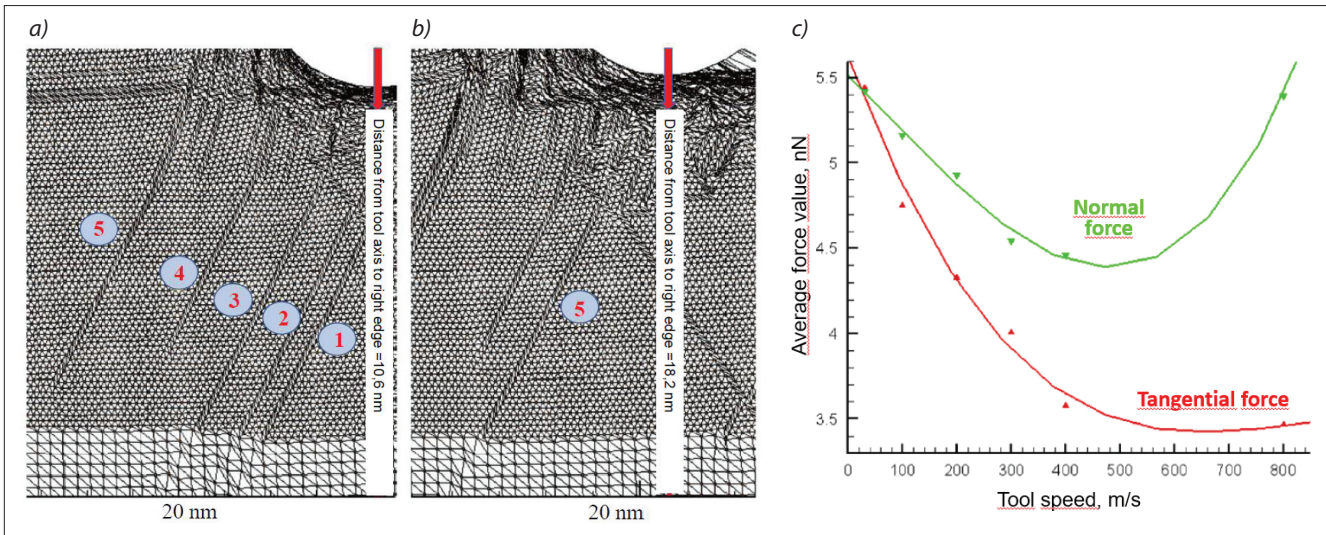


Fig. 5. Distribution of dislocations in the material under compression (a) and after relaxation (b) determined using multiscale modeling of (MD+FEM) type and forces distribution in the scratch test vs. tool speed (c) [4, 7]

shear stress values are 11,000 MPa and 29.0 MPa [5], respectively. There are edge, screw, and mixed dislocations; however, in real crystals, there are mixed dislocations with varying contributions of edge and screw components. Dislocation transitions through the crystal are the basic mechanism causing continuous deformations. Therefore, microstructure modelling should take into account the movement of dislocations, as in fig. 2.

From the slip band model presented in fig. 4, a dimensionless measure of the degree of plastic deformation—called the shear strain—is determined as $\gamma = \Delta s/d$.

The mechanism of slipping at the micro- and nanoscale is explained based on molecular simulations (MD) or by using a two-scale model (MD+FEM) that considers the effect of dislocations [4, 7, 8]. In the case of highly plastic metals, such as pure copper and aluminium, a continuous and stable chip of a few nanometres in thickness is removed, similar to conventional cutting, but the components of cutting force, cutting temperature, vibrations, and wear of the diamond tool are three to four orders of magnitude smaller [4]. Fig. 5 shows the distribution of

dislocations in the atomic zone of the material subjected to compression (fig. 5a) and after relaxation (fig. 5b) in two time intervals after the scratch test. The numbers 1–5 mark visible slip lines related to the path of dislocation movement in the atomic zone. The scratch depth was 2.0 nm, and the displacement of the stylus was 100 nm/s. The penetration of at least five dislocations into the material and the penetration of dislocations numbered 1–3 into a continuous area of continuum character are clearly visible. In turn, fig. 5b shows that with the progress of the tool movement, at least four out of five marked dislocations experience reverse slip and disappear on the free surface. These observations indicate that the internal area of the material adjacent to the slip plane does not show a characteristic concentration of slip stresses but is subjected to almost constant and large compressive stresses. This confirms the role of high hydrostatic stresses in facilitating slipping, which is commonly observed in the cutting process [5]. Fig. 5c shows the distribution of normal and tangential forces as a function of tool (indenter) speed obtained from data collected during grooving with a depth of

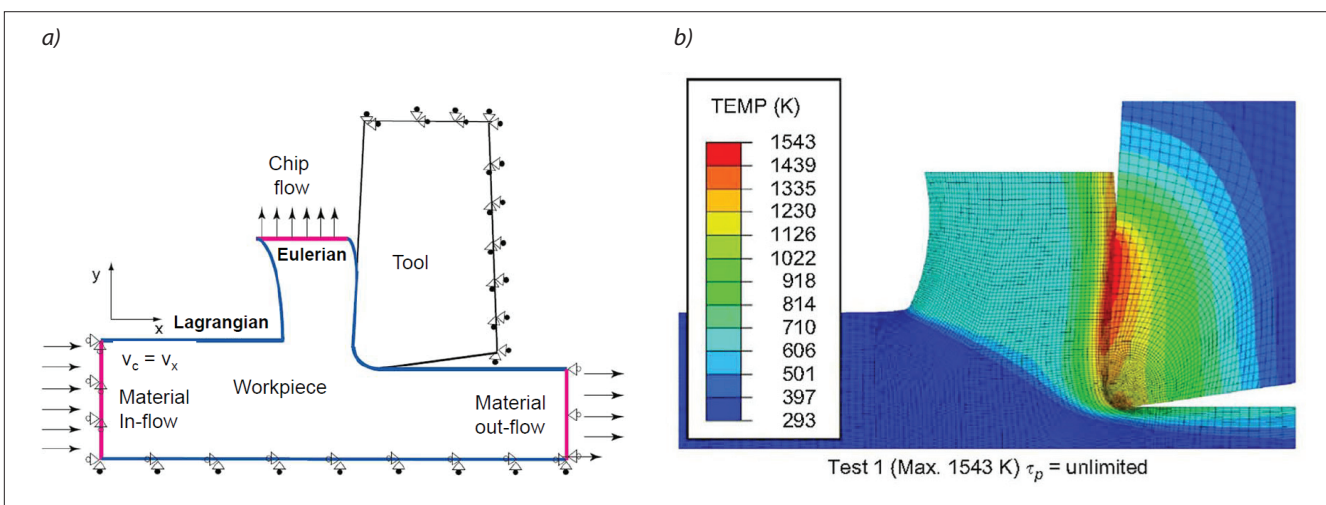


Fig. 6. Scheme of the coupled FEM Eulerian-Lagrangian (ALE) model for orthogonal cutting (a) and generated thermal map in the cutting zone (b) [9]

2.0 nm over a length of 100 nm. It is clear from fig. 5c that outside the range of plastic flow wave propagation, the force values decrease rapidly (approximately above 300 m/s), which corresponds well with the transition region from dislocation-induced plastic flow of the material to the amorphous crystal state.

Finite Element Method and Hybrid FEM-SPH/FEM-DM Simulation

In modelling the cutting process, the most commonly used FEM methods are the Lagrangian, Eulerian, or ALE (Arbitrary Lagrangian–Eulerian) approaches [4, 5], along with many commercial software packages, e.g. DEFORM, ABAQUS, ANSYS, and AdvantEdge. In order to obtain reliable simulation results, appropriate input data must be provided, including the constitutive equation and suitable finite element mesh fitting the specific research object. Fig. 6 shows a scheme of the combined FEM simulation of the cutting process, where the tool model is presented in the Lagrangian domain and the removed material layer in the Eulerian domain [9].

This combined FEM model configuration enables discretisation of the tool with a mesh size of 0.005–0.1 mm and a smaller mesh size of 0.005–0.05 mm in the region where material is transformed into a chip. The simulation was carried out as a 3D model using the ABAQUS/Explicit software package. An example of the application of the FEM ALE method for determining the temperature distribution (thermal

map) in the cutting zone when turning AISI 4340 steel with an uncoated carbide tool is shown in fig. 6b.

In practice, though on a smaller scale, FEM simulation is used with large spatial elements—so-called voxels—instead of the classic finite element mesh, which allows for determining the deformation of the entire object during machining. Meshless modelling methods of the SPH type (*Smooth Particle Hydrodynamics*) and hybrid FEM-SPH methods [4, 8, 9, 10] are also employed.

An example of a hybrid 2D orthogonal cutting model, consisting of an SPH particle mesh (upper part) and an FEM mesh (lower part), which considers the convergence of these two approaches, is shown in fig. 7a. A plane strain model was adopted, described by a Johnson–Cook (JC) type constitutive equation and a cumulative damage (decohesion) model of the D type material [5]. This means the motion of the SPH particles and the FEM mesh elements is completely constrained in the Z-axis direction.

Fig. 7b shows the results of the 2D simulation of the segmented chip formation model in the orthogonal cutting of the alloy aluminium A2024-351 with the imaging of the distribution of the degree of strain (*effective plastic strain*) and the damage variable. The problem in 2D modelling using the (SPH+FEM) method is the relatively low efficiency of calculations and the accuracy of the prediction of cutting force components, of the order of 50%. For this reason, in 3D models that require a very large number of SPH particles, the actual cutting speed is intentionally overestimated by a factor of 5, 10 or 20-times in order to reduce the simulation time [4].

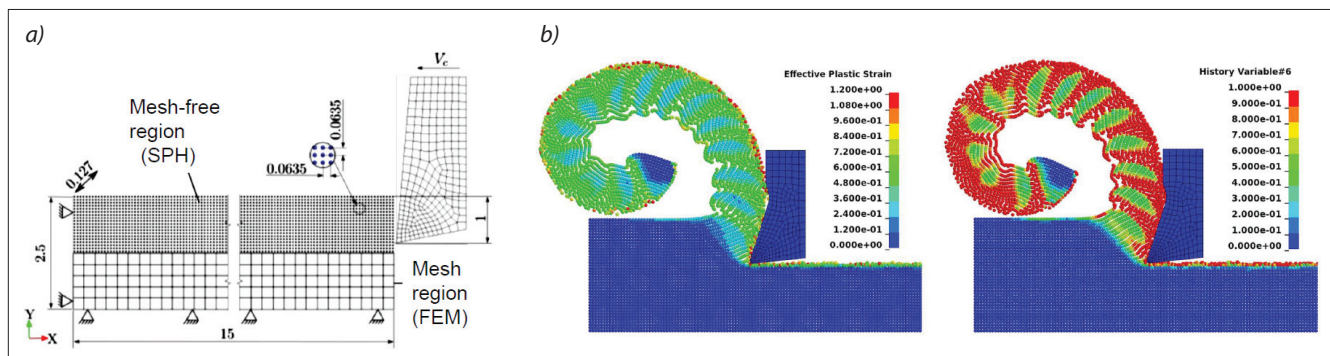


Fig. 7. 2D simulation model of orthogonal cutting using the (SPH+FEM) method, showing model geometry and boundary conditions (a), and 2D simulation of segmented chip formation showing the distribution of effective plastic strain and damage variable (b) [9, 10] and method concept according to [20]

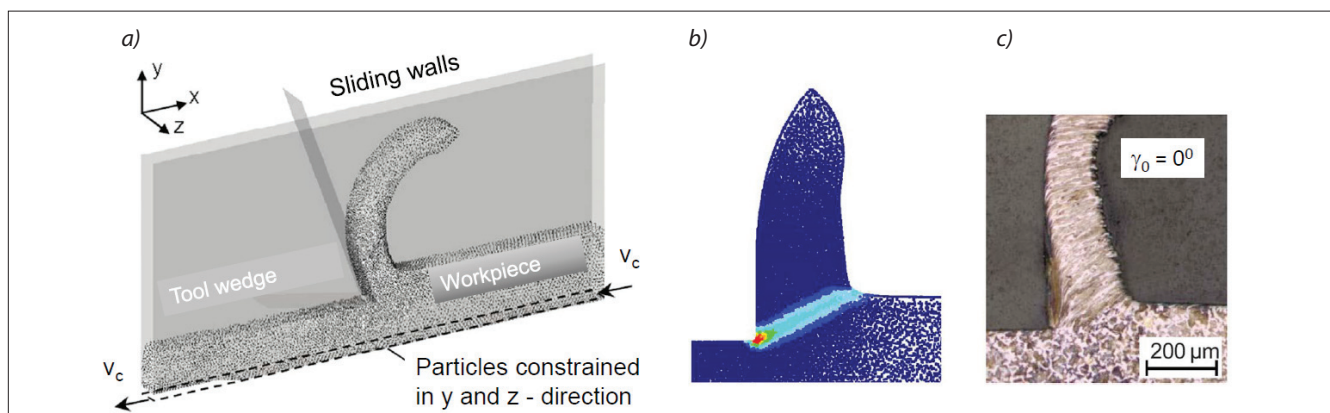


Fig. 8. An FPM model for orthogonal machining of Inconel 718 (a), FPM simulation (b), and experimental result of chip formation (metallographic image of the chip root) (c) [9]

Fig. 7c illustrates the concept of hybrid simulation of the cutting process based on the combination of the SPH technique for the workpiece and the FEM for the tool materials. To determine the temperature distribution in the cutting zone of Ti6Al4V alloy with a WC-Co tool, a new method of heat transfer between component models was developed. By precisely defining thermal contact at the chip-tooth contact surface, good agreement was achieved with the results of commercial FEM simulation and experimental measurements. The calculations were performed on a GPU (Graphics Processing Unit) to accelerate the computation. The Finite Pointset Method (FPM) shares some similarities with the previously discussed SPH method. In the 2D FPM model shown in fig. 8a, free particles are clearly visible instead of a typical FEM mesh. Notably, the tool model is rigid (fixed), and there is no heat exchange with the environment, which differs from the classical FEM method (fig. 6a). The simulation result is illustrated in fig. 8b, showing the geometry of the chip formation zone compared to the actual chip root tool the quick-stop device.

Modelling of the micro and nano machining process

Research on the ultra-precision machining process belongs to the dynamically developing, largely new branch of machining called *micro-cutting/nano-cutting* [1, 5, 6]. In nano-cutting, typical values of the cutting layer thickness are less than 1 μm , and sometimes even 1 nm, while the radius of the rounding of the edge of a single-crystal diamond tool is in the range of 1.5–4.5 nm.

In micro-/nano-cutting, the possibility of stock removal results from *the scale effect*, which can be interpreted in three ways, i.e. as an effect of the cutting edge radius scale, the material microstructure scale and the material properties [4, 8]. The first case concerns a very small value of the h/r_n ratio, the second when the grain size is comparable to the radius of the

cutting edge rounding/the thickness of the cutting layer, and the third when the ratio of the size of the machined part fragment to the grain size is close to 1 or the ratio of its surface area to volume increases. The effect of these limitations is a strong dependence of plastic deformations on the mobility of dislocations and there is a need to include dislocations in the deformation mechanism, as in Fig. 4 [4, 5, 6].

The modelling and simulation of the micro-/ nano-cutting process is performed using the finite element method (FEM/MES), especially the ALE (*Arbitrary Lagrange-Euler*), molecular dynamics (MD) and multi-scale simulation (MS) [4, 9]. FEM simulation, e.g. of the micro-milling process, is performed in a similar way to the traditional process, except that much attention is paid to the formation of micro-burrs, component forces and heat generation. In the studies of the micro-/nano-cutting process, special attention is paid to the influence of the rounding (sharpness) of the cutting edge on the formation of chips and the formation of surface roughness. Experimental studies and computer simulation using the molecular dynamics (MD) method are carried out, together with 3D graphic visualization software (VMD – *visual molecular dynamics*) [4, 9]. The MD method is basically limited to structures composed of a few million atoms and time scales down to picoseconds and for this reason it is the dominant tool in nanoscale simulations [5, 8, 12]. In the experimental phase, the course of plastic deformations is observed on a scanning microscope, which is mounted on ultra-precision, miniature lathe with *in situ* measurement of tool setting, coupled. Computer simulation includes analysis of stresses, strains, material flow and generated heat.

Fig. 9a shows the model of cutting a single copper crystal with a single diamond tool for the dimensions of the workpiece with the multiple of the atomic lattice constant (a), which is built of *edge, thermostatic and Newtonian atoms*. Thermostatic atoms conduct and remove the generated heat. The entire model of the workpiece in fig. 8a contains 43,240 copper atoms

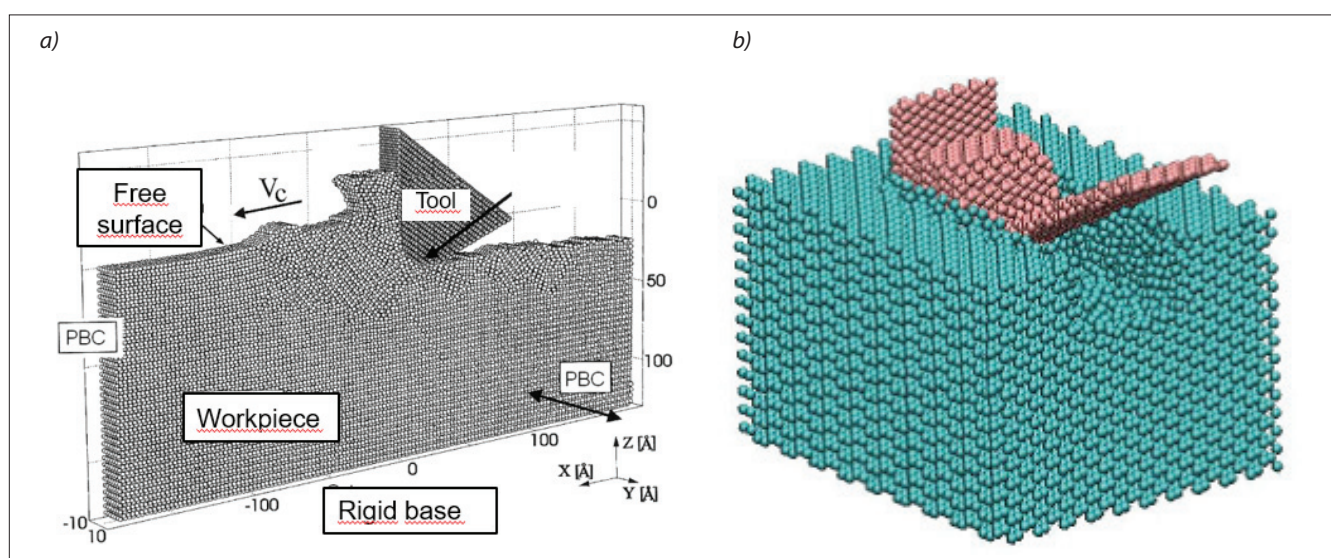


Fig. 9. MD simulation of machining performance of single copper crystal (a) and atomic scale cutting model of pure copper/aluminium and monocrystal SIC using diamond monocrystal tool (b) [4, 5, 12]. PBC – Periodic Boundary Conditions

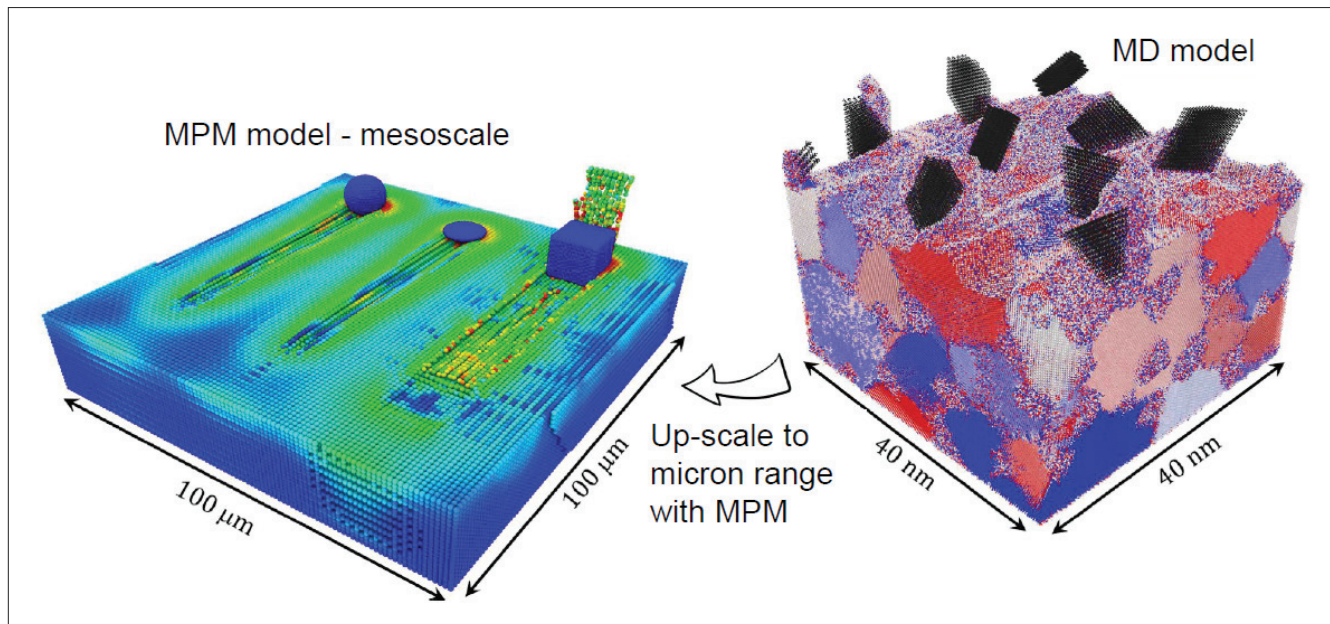


Fig. 10. Grinded workpiece and machined surface generation using (MD+MPM) multiscale modeling system [16]

with an *fcc crystal lattice*, and the tool model contains 10,992 carbon atoms with a diamond structure. In turn, fig. 9b shows an analogous model used for nano-cutting of single-crystal SiC. Based on the MD simulation carried out for three values of the cutting edge radius (0.5, 1.5 and 5 nm), it was determined that the minimum thickness of the cutting layer measured with technically achievable accuracy was about 1 nm, i.e. $1/20^{-1}/10$ of the radius of the cutting edge rounding,

while the process itself is more energy-intensive because about 50% of the energy is used for deforming the material under the tool, which is much more than on a macro scale [4, 5].

A significant reduction in simulation time (even threefold) is achieved using the ARMD (*area-restricted molecular dynamics*) based on limiting the area of molecular dynamics simulation. The simulation was based on the model of dislocation movement in the

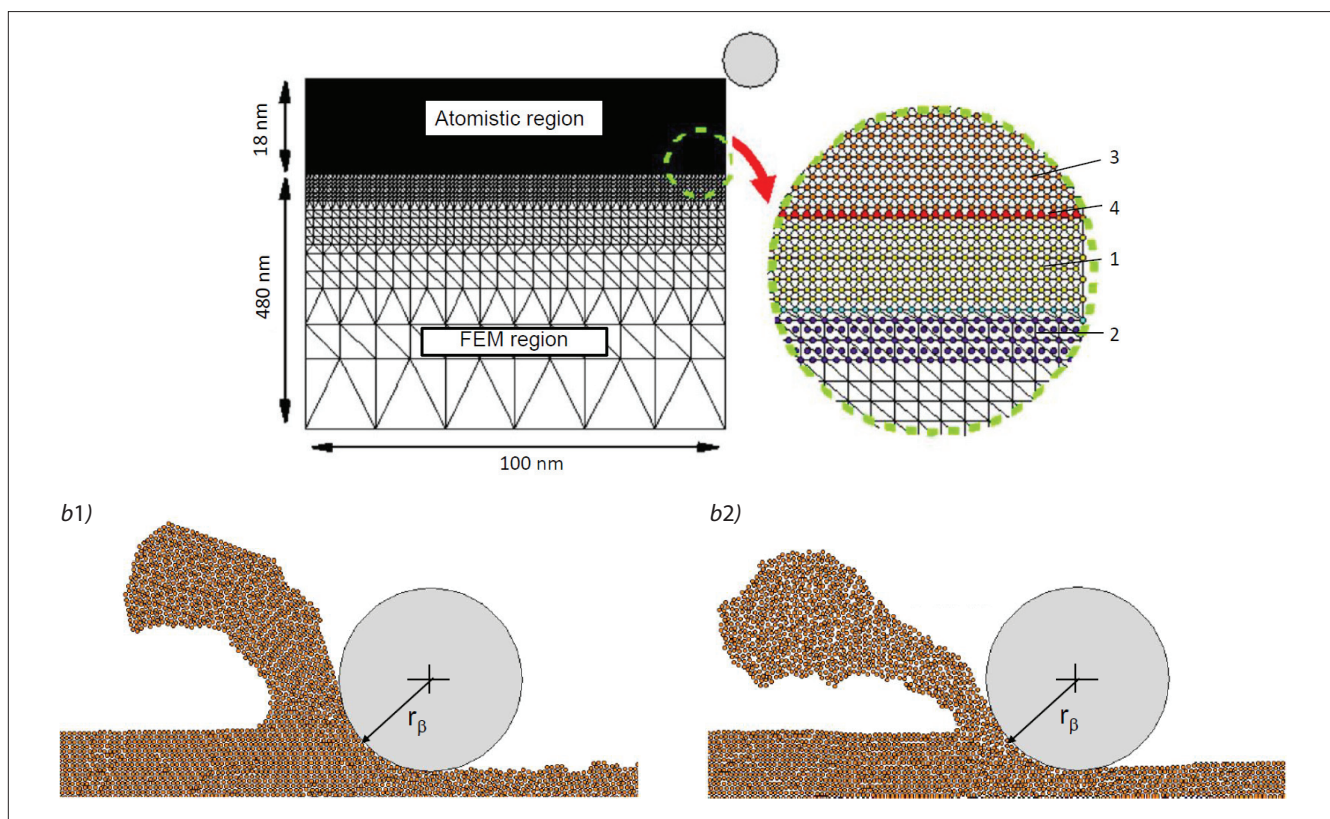


Fig. 11. Multiscale model geometry and a close-up of the atomistic/continuum interface which shows continuum elements, atoms, pad atoms and interface atoms (a) and close-up of chip profile for two different tool speed: (b1) 200 m/s; (b2) 800 m/s [7]. Symbols in Fig. 9a: 1 – the atom/nodes created the actual interface between the two regions, 2 – mesh elements that lie inside the continuum region created a “pad” of atoms to couple the atoms to the continuum region, 3 – detection elements, 4 – atoms located in damping band region. The depth of scratching is equal to 2.0 nm

slip zone assuming the existence of *zig-zag dislocation movement*, which consists in their transition from the area of contact of the material with the tool, through the slip zone, to the free surface. Based on the simulation of the displacement trajectories of *working atoms* and instantaneous values of the temperature of each of the atoms in a cycle of 60,000 steps (corresponding to a tool displacement of approx. 12 nm), it was established that the chip formation at the nanoscale is similar to that observed during micro-cutting.

In the case of grinding a workpiece made of nanocrystalline carbon steel with a content of 1.7 wt % C, in the first phase, the microstructure model with the initial polycrystalline ferritic structure was supplemented with cementite (Fe_3C) grains as the second phase using the MD method, approaching the macroscopic level, as in Fig. 10. The initial 3D-periodic system of dimensions $85 \times 85 \times 85 \text{ nm}^3$ containing about 200 randomly oriented grains generated in the Dream.3D microstructure program was imported to the Matlab simulation package. Then, using the MD method on a larger scale, the grinding process was simulated with micro-grains of aluminium oxide

$\text{a-Al}_2\text{O}_3$, which were placed above the workpiece surface. The particle system was visualized in the OVITO program. In the next step, a model of the formation of surface microtopography in the mesoscale (fig. 9a) was generated using the meshless MPM (*material point method*). In this case, the chip formation and process efficiency were observed to be correctly reproduced on a large scale. This approach allows the process to be optimized with respect to the efficiency and surface quality criteria.

In turn, the *micro-scale model*, and often even *nanoscale model*, is used to study changes occurring in the material during the process, e.g. changes in microstructure, hardness or dislocation movement, the so-called multi-scale modelling (MD+FEM) is used, which consists in combining the molecular dynamics method (MD-*molecular dynamics*) with the classical finite element method (FEM-*finite element method*). Fig. 11a shows the geometry of the hybrid multi-scale model (MD+FEM) with the atomistic boundary and continuum containing continuous elements of the FEM mesh, atoms, substrate/pad atoms and atoms on the interface of submodels. Fig. 11b shows the formation of

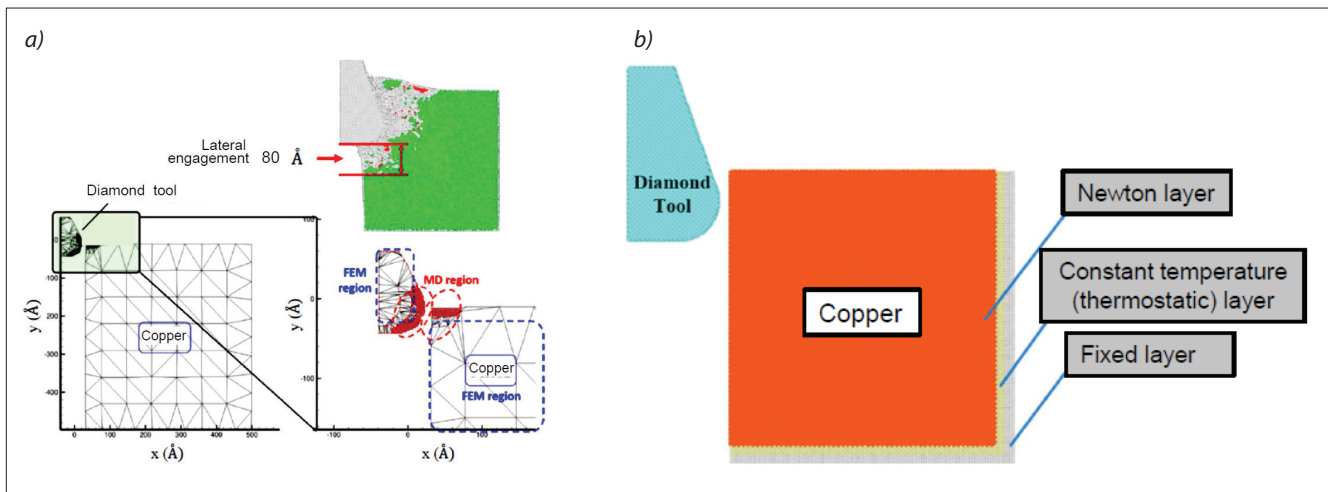


Fig. 12. A scheme of multiscale model of nanomachining of samples made of pure copper (a) and sample layer structure (b) [4, 15]

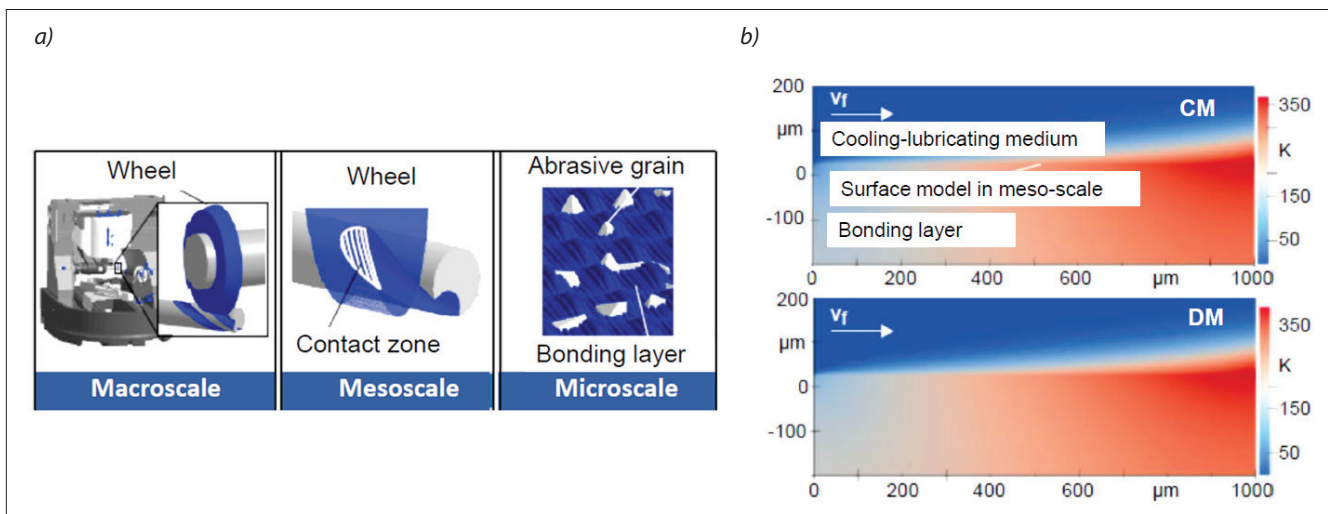


Fig. 13. Methodology of multiscale modeling of tungsten carbide grinding with PCD wheel (a) and temperature distribution in the mesoscale determined by means of CM and DM modeling techniques (b) [19]

a chip at a speed of 200 m/s and 800 m/s and a depth of 2.0 nm. Plastic deformations caused by the presence of slip lines are visible. The chips created have a polycrystalline (b1) or amorphous (b2) structure, depending on the cutting speed.

Fig. 12 shows a scheme of the multiscale model of nano-cutting of a pure copper sample, which combines FEM and MD modelling [4, 7, 13, 14]. It can be easily observed that the contact zone between the tip and the sample is modelled as an atomic region (MD region), while the remaining zone is covered by the FEM model. In this way, the initial multiscale model was reduced to the $500\text{\AA} \times 500\text{\AA} \times 4a$ (a is the Cu atomic lattice constant in the *fcc* structure equal to 3.62) with about 510 atoms instead of 250,000 atoms in the classical MD model. The diamond tool is a rigid body moving with a velocity of 1 /ps [13].

Fig. 13a shows the thermal simulation methodology of the grinding process of porous carbide blade inserts with a PCD grinding wheel ($v_c = 10$ m/s, $v_f = 1486$ mm/min) in the presence of a cooling-lubricating liquid and the generated thermal maps (fig. 13b), when the CM (*continuous model of temperature field*) and DM (*discontinuous model of temperature field*) methods were used for the micro/ meso-scale simulation [19]. The active surface of the grinding wheel was created from diamond styluses used in *scratch* tests with a maximum diamond grain size of 180 μm surrounded by a Cr-Cu bonding coating. It can be seen that the continuous model (CM) taking into account all abrasive grains leads to the determination of a lower energy expenditure than the discrete model (DM). The problem is to determine the appropriate parameters describing the flow and heat exchange in the porous material-abrasive grain system. It is possible to determine appropriate thermal maps in the micro scale for a single abrasive grain [19]. A similar modelling methodology (based on the Reynolds flow equation) was used to assess the penetration of CCS into the chip-tooth contact zone [21].

The presented directions of development and application of large-scale modelling and hybrid simulation techniques of the microstructure of the processed material and the course of the process developed on this basis seem to be future solutions due to their practically unlimited possibilities in the selection of the scale of description of physical phenomena - from atomic to macroscale. Additionally, they enable simulation in time acceptable in engineering research and analysis [23, 24].

More information on the usefulness of large-scale modelling in plastic, additive and hybrid processing can be found in review articles and books [3, 17, 22].

REFERENCES

- [1] Lin, K., and Z. Wang. „Multiscale Mechanics and Molecular Dynamics Simulations of the Durability of Fiber-Reinforced Polymer Composites.” *Communications Materials*, vol. 4, 2023, p. 66, <https://doi.org/10.1038/s43246-023-00391-2>.
- [2] Gohari, H., et al. „High-Performance Machining System: Process Optimization for a Cyber-Physical System – A Review.” *Preprints.org*, 2024, doi:10.20944/preprints202401.1951.v1.
- [3] Yanagimoto, J., et al. „Simulation of Metal Forming. Visualization of Invisible Phenomena in the Digital Era.” *CIRP Annals - Manufacturing Technology*, vol. 71, 2022, pp. 599-622.
- [4] Grzesik, W., et al. *Analysis and Modelling of Surfaces Produced by Subtractive Machining*. PWN, 2024.
- [5] Grzesik, W. *Advanced machining processes of metallic materials*, Elsevier, 2017.
- [6] Madej, Ł., and M. Sitko. „Computationally Efficient Cellular Automata-Based Full-Field Models of Static Recrystallization: A Perspective Review.” *Steel Research International*, vol. 1, 2022, doi:10.1002/srin.202200657.
- [7] Shiaria, B., R. E. Miller, and D. D. Klug. „Multiscale Simulation of Material Removal Processes at the Nanoscale.” *Journal of the Mechanics and Physics of Solids*, vol. 55, 2007, pp. 2384–2405.
- [8] Cheng, K., and D. Huo. *Micro-Cutting. Fundamentals and Applications*. Chichester, 2013.
- [9] Melkote, S., et al. „A Review of Advances in Modeling of Conventional Machining Processes: From Merchant to the Present.” *Journal of Manufacturing Science and Engineering*, vol. 144, 2022, pp. 110801-11–110801-22.
- [10] Ojal, N., et al. „A Realistic Full-Scale 3D Modeling of Turning Using Coupled Smoothed Particle Hydrodynamics and Finite Element Method for Predicting Cutting Forces.” *Journal of Manufacturing and Materials Processing*, vol. 6, no. 2, 2022, p. 33, doi:10.3390/jmmp6020033.
- [11] Hardt, M., et al. „On the Application of the Particle Swarm Optimization to the Inverse Determination of Material Model Parameters for Cutting Simulations.” *Modeling*, vol. 2, 2021, pp. 129–148, doi:10.3390/modelling2010007.
- [12] Jain, V. K. *Micromanufacturing Processes*. CRC Press, 2013.
- [13] Xu, Y., et al. „Multiscale Assessment of Nanoscale Manufacturing Process on the Freeform Copper Surface.” *Materials*, vol. 13, 2020, p. 3115, doi:10.3390/ma13143135.
- [14] Pratap, A., et al. „Understanding the Surface Generation Mechanism during Micro-Scratching of Ti-6Al-4V.” *Journal of Manufacturing Processes*, vol. 82, 2022, pp. 543–558, doi:10.1016/j.jmapro.2022.08.014.
- [15] Xu, Y., et al. „Multiscale Assessment of Nanoscale Manufacturing Process on the Freeform Copper Surface.” *Materials*, vol. 13, 2020, p. 3135, doi:10.3390/ma13143135.
- [16] Eder, S. J., et al. „A Multiscale Simulation Approach to Grinding Ferrous Surfaces for Process Optimization.” *International Journal of Mechanical Sciences*, vol. 194, 2021, p. 106186.
- [17] Teimouri, R. „Multiscale Modeling of a Chain Comprising Selective Laser Melting and Post-Machining Toward Nanoscale Surface Finish.” *Materials*, vol. 16, 2023, p. 7535, <https://doi.org/10.3390/ma16247535>.
- [18] „Multiscale Modeling Techniques.” *ETH Zurich*, <https://mm.ethz.ch/education/master-phd-studies/multiscale-modeling.html>.
- [19] Wiesener, F., et al. „Modeling of Heat Transfer in Tool Grinding for Multiscale Simulations.” *Procedia CIRP*, vol. 117, 2023, pp. 269–274, doi:10.1016/j.procir.2023.03.046.
- [20] Zhang, N., et al. „Hybrid SPH-FEM Solver for Metal Cutting Simulations on the GPU Including Thermal Contact Modeling.” *CIRP Journal of Manufacturing Science and Technology*, vol. 41, 2023, pp. 311–327, doi:10.1016/j.cirpj.2022.12.012.
- [21] Sauer, F., et al. „Multiscale Simulation Approach to Predict the Penetration Depth of Oil between Chip and Tool during Orthogonal Cutting of AISI 4140.” *Procedia CIRP*, vol. 117, 2023, pp. 426–431, doi:10.1016/j.procir.2023.03.072.
- [22] Zhang, Y., et al. *Multiscale Modeling of Additively Manufactured Metals*. Elsevier, 2020.
- [23] Grzesik, W. „Progress in Modelling and Simulation of the Machining Process – Part I: Multiscale Modelling.” *Mechanik*, no. 3, 2024, pp. 30–37, doi:10.17814/mechanik.2024.3.4.
- [24] Grzesik, W. „Progress in Modelling and Simulation of the Machining Process – Part II: Mesh-Free Modelling and Simulation.” *Mechanik*, no. 5-6, 2024, pp. 6–15, doi:10.17814/mechanik.2024.5-6.9. ■